Published in Journal Electroanalytical Chemistry 2010, vol 638, p 131-142
DOI: 10.1016/j.jelechem.2009.10.008

The impact of high Zn⁰ concentrations on the application of AGNES to determine free Zn(II) activity

Josep Galceran*, Diana Chito, Neus Martínez-Micaelo, Encarnació Companys, Calin David and Jaume Puy

Departament de Química. Universitat de Lleida, Rovira Roure 191, 25198 Lleida, Spain

• corresponding author galceran@quimica.udl.cat

Abstract

AGNES (Absence of Gradients and Nernstian Equilibrium Stripping) determination of free Zn(II) in a solution can be affected by the reaching of high Zn⁰ concentrations inside the amalgam. At concentrations about the solubility limit of Zn⁰ in mercury, the formation of dendrites and powders around the mercury surface can be seen with an optical microscope. At concentrations of Zn⁰ quite below the solubility limit, an anomalous stripping current appears which increases with decreasing supporting electrolyte concentration. The current along the stripping time exhibits a convex shape, which is labelled here as "anomalous convex behaviour" (acb). The origin of acb is tentatively ascribed to different kinetic reasons (amongst which the electroneutrality limitation due to low ionic strength outstands), but more than one cause is necessary for a full account of the experimental observations. With various strategies, like monitoring the charge as response function or by application of lower gains, AGNES can successfully probe these high concentrations.

Keywords: AGNES, stripping analysis, amalgam, free metal.

1. Introduction

AGNES (Absence of Gradients and Nernstian Equilibrium Stripping) is an emerging electroanalytical technique specifically designed to determine free metal concentrations [1]. Its application to a variety of systems, ranging from synthetic solutions to Mediterranean seawater, has been extensively validated on theoretical grounds or with consolidated techniques such as Ion Selective Electrode, Resin Titration or Scanned Stripping Chronopotentiometry [2-9]. The key idea of AGNES is the preconcentration of reduced metal (Zn^0 in this work) inside the amalgam up to the equilibrium value (set by the applied potential and Nernst equation). The determination of the amount of Zn^0 at equilibrium has been performed, up to now, via the stripping current under diffusion limited conditions. At large concentrations of the reduced metal (and low ionic strength), we have observed a current distortion, which might hinder the standard application of AGNES in some systems (for instance, in determining the complexation capacity of wine with the standard HMDE [4] or when working with film electrodes [9]).

A distortion of the current is clearly expected when the solubility limit of Zn^0 inside the amalgam is exceeded (5.8% in atomic percentage [10], approximately 4 M, at 25ºC). It is obvious that stripping currents for aimed Zn^0 concentrations larger than the solubility limit could not be used for the analytical general purpose of AGNES. But, a literature search indicates that problems might appear well before. For instance, Arevalo et al. [11] found a linear behaviour of the stripping current with $[Zn^0]$ at least up to $[Zn^0]=3\times10^{-3}$ M, while reporting that Babkin had found that the linear relationship ceased from $[Zn^0]=1.2\times10^{-2}$ M onwards (the current increased more rapidly than $[Zn^0]$). Moreover, a long tradition of literature [12-15] has pointed out that there might be "kinetic" problems: even at reduced metal concentration globally lower than the

solubility limit, during the deposition there might be spots (in the amalgam, close to the surface of the interphase) where the local concentration exceeds the solubility limit and forms deposits. More recently, experimental and theoretical evidences (with Tl) indicate that the stripping currents are strongly influenced by low supporting electrolyte concentrations [16,17].

The outline of this article is as follows. We summarize AGNES methodology and introduce two new concepts: i) the time-function η, expressing the direct proportionality between stripping current and reduced metal concentration, which allows for diagnosing anomalous behaviours and ii) the charge as response function in AGNES. We describe the case of formation of Zn° deposits around the mercury drop linking optical and electrochemical information. We study the deviation from the current-concentration linearity, consider various hypotheses which might participate in the justification of the experimental results and describe practical strategies to apply AGNES when dealing with high concentrations.

2. The principles of AGNES

AGNES is a stripping technique whose novel idea is the attainment of a special situation of equilibrium by the end of the deposition stage [1]. The sought equilibrium can be achieved by application of a deposition potential E_1 for a sufficiently long time t_1 (see table 1). E_1 is usually just a few millivolts more negative than the standard formal potential of the couple $E^{0'}$, so that the prescribed gain Y, attained by the end of the deposition stage and given by Nernst law,

$$Y = \frac{[\mathrm{Zn^o}]}{[\mathrm{Zn^{2+}}]} = \exp\left[-\frac{2F}{RT}\left(E_1 - E^{0'}\right)\right] \qquad (1)$$

is moderate. F is the Faraday, R the gas constant, T the temperature and the concentrations refer to the homogeneous profile (i.e. absence of gradients) inside the mercury electrode and in the solution. [Zn°] in this article refers exclusively to the bulk homogeneous concentration obtained inside the drop by the end of the first stage, so that it is not a time-dependent variable.

Up to this work, the only response function of AGNES considered has been the intensity current at a fixed time t_2 (within the stripping stage) which is sought to be under diffusion limited conditions (with a stripping gain Y_2 computed with eqn (1), but replacing E_1 with E_2, a much more positive potential used for the reoxidation stage). These conditions, due to the linearity of the continuity equation for Zn° inside the amalgam (see appendix in [1]), ensure that the faradaic current I (obtained from the measured current once a suitable blank has been subtracted) is proportional to [Zn°]:

$$I = \eta \left[\mathrm{Zn^o} \right] \tag{2}$$

where the new proportionality factor η only depends on the elapsed time of the stripping step (which –for simplicity- we also label t_2) and on the characteristics of the diffusion of Zn° in the amalgam (diffusion coefficient and shape and size of the drop). The plot of

$$\eta(t_2) = \frac{I(t_2)}{\left[\mathrm{Zn^o} \right]} = \frac{I(t_2)}{Y\left[\mathrm{Zn^{2+}} \right]} \tag{3}$$

along the stripping time should be the same –for a fixed electrode and metal- regardless of Y and [Zn^{2+}]. In order to control deviations in the stripping current from the expected linear behaviour, we will plot $\eta(t_2)$, to which we will refer here as "plot of normalised currents". The "reference curve" will be given by the collapse of all plots of $\eta(t_2)$ at conditions with no anomalies (usually low metal concentrations and high ionic strength).

Combining eqns. (1) and (2), we can write

$$I = \eta\left[\mathrm{Zn^o}\right] = \eta Y\left[\mathrm{Zn^{2+}}\right] = h\left[\mathrm{Zn^{2+}}\right] \quad (4)$$

where $h(t_2)$ is the proportionality factor between the experimental faradaic current and the sought free metal concentration in the solution bulk. For analytical purposes, h can be determined from a calibration plot and, then, used with the faradaic current measured in the studied sample.

Alternatively to the use of the intensity current (at a fixed t_2), we explore here the use of the deposited charge. Indeed, by simple integration of eqn. (2) along the (complete) stripping time:

$$Q = \int_0^\infty I\, dt_2 = \int_0^\infty \eta\left[\mathrm{Zn^o}\right] dt_2 = \left(\int_0^\infty \eta\, dt_2\right)\left[\mathrm{Zn^o}\right] = \eta_\mathrm{Q}\left[\mathrm{Zn^o}\right] \quad (5)$$

where we have added a subscript Q to indicate that the proportionality refers to the charge (and not to the current, as usual). η_Q can be related to the volume of the electrode. If we assume a spherical electrode of radius r_0:

$$\eta_\mathrm{Q} = 2F\,{}^4\!/_3\,\pi r_0^3 \quad (6)$$

Combining eqns. (1) and (5), we can write

$$Q = \eta_\mathrm{Q}\left[\mathrm{Zn^o}\right] = \eta_\mathrm{Q} Y\left[\mathrm{Zn^{2+}}\right] = h_\mathrm{Q}\left[\mathrm{Zn^{2+}}\right] \quad (7)$$

If one has determined η_Q from a calibration plot, further charge measurements in a sample solution can yield its free metal concentration:

$$\left[\mathrm{Zn^{2+}}\right] = \frac{Q}{Y\eta_\mathrm{Q}} \quad (8)$$

In principle, one could use any measure of the faradaic charge (i.e. in the first or second stage), but we have noticed that the stripping charge is much more reproducible than the deposition charge, and, so, in this work, Q always refers to the charge measured in the stripping stage.

3. Materials and Methods

3.1 Reagents

Zinc and cadmium stock solutions were prepared from $Zn(NO_3)_2.4H_2O$ and $Cd(NO_3)_2.4H_2O$ (Merck, analytical grade), respectively, and standardised by means of a complexometric endpoint titration with EDTA [18]. Diluted solution of Zn and Cd were prepared from the Zn and Cd stock solutions, respectively, or from Zn and Cd 1000 mg/L standard solution (Merck). Potassium nitrate was used as inert supporting electrolyte and prepared from solid KNO_3 (Fluka, TraceSelect). The ionic strength has been mainly fixed at 0.05 M (because of the interest of wine matrices [4,19,20]. Titrisol (Merck) or standard 0.1 M solutions (Riedel de Haen) of KOH and HNO_3 were added to fix the pH at the desired values. Mercury (Fluka p.a.) was used in the working electrode.

Ultrapure water (Milli-Q plus 185 System, Millipore) was employed in all the experiments. Purified water-saturated nitrogen $N_2(50)$ was used for deaeration and blanketing of solutions.

3.2 Instrumentation

Voltammetric measurements were carried out with Eco Chemie Autolab PGSTAT30 PGSTAT12 or PGSTAT10 potentiostats attached to a Metrohm 663 VA Stand and to a computer by means of the GPES 4.9 (Eco Chemie) software package. The working

electrode was a Metrohm multimode mercury drop electrode. The smallest drop in our stand has been chosen, which, according to the catalogue, corresponds to a radius around r_0= 1.41×10^{-4} m. This size was confirmed by measurements with our microscope. The auxiliary electrode was a glassy carbon electrode and the reference electrode was Ag | AgCl | (3 mol L^{-1}) KCl, encased in a 0.1 mol L^{-1} KNO_3 jacket.

A glass combined electrode (Orion 9103) was attached to an Orion Research 720A Ionanalyzer and introduced in the cell to control the pH (all the experiments were performed at pH in the range 3-5). Glass jacketed cells (thermostated at 25.0ºC) provided by Metrohm or Afora were used.

To monitor the evolution of the mercury drop, a CCD digital camera (Lumenera INFINITY2-1) was coupled to a microscope Navitar Zoom 6000 (with coaxial illumination), following previously reported designs [21]. To obtain a large magnification range (6.96x – 228.6x), two different objective lenses (10x and 50x, working distances 33 mm and 13 mm respectively) were used. A linear motor positioning stage (Standa, Lithuania) controlled by a microstep stepping motor driver was used to move the microscope in 3D with a resolution of ca. 0.16μm. A flat quartz window was added to a double-wall voltammetric cell.

3.3 Procedures

AGNES experiments were applied with the simplest potential program, i.e. a fixed constant potential during the deposition step (see [1] for more details). The standard response function of AGNES has been the value of the current at a certain time t_2 in the reoxidation step (e.g. 200 ms for these experiments with this HMDE). As an alternative

source of information, we compute the charge along the reoxidation step by just integrating the current measured along the second stage using the trapezoid rule (and a zero current for t_2=0, which will imply an underestimation of the actual charge):

$$Q = \int_0^{\infty} I \, dt_2 \approx \Delta t \left(\sum_{j=1}^{n_{\max}} I_j \right) \qquad (9)$$

where Δt is the sampling time (either 1 ms or 50 ms), I_j is the faradaic current at a given measurement point j corresponding to the variable time t_2 (i.e. $j = t_2/\Delta t$). The faradaic current has been obtained by subtracting a blank current (usually negligible in these experiments) and I_∞ (which is the residual current, average of the measured current around the end of the second stage). Typically, the stripping stage lasted 50 s, so that the standard maximum number of points is $n_{\max}$= 50/0.050=1000. Due to the discretization, the actual value of Q –and the ensuing parameters h_Q and η_Q- depends on the experimental interval time Δt, converging to a fixed value for low enough Δt.

In order to estimate an upper bound for the maximum possible charge in a stripping stage with standard behaviour, we have assumed cottrellian behaviour up to the first sampled point (whose current is labelled here as I_1), given that sphericity and finite volume effects can be considered negligible for that time. Then, the maximum charge up to the first sampled point should be

$$Q_1 = \int_0^{\Delta t} I \, dt = \int_0^{\Delta t} 2F 4\pi r_0^2 [\mathrm{Zn^o}] \sqrt{\frac{D_{\mathrm{Zn^o}}}{\pi t}} \, dt = 2 \times 2F 4\pi r_0^2 [\mathrm{Zn^o}] \sqrt{\frac{D_{\mathrm{Zn^o}} \Delta t}{\pi}} = 2 \, I_1 \, \Delta t \qquad (10)$$

where $D_{\mathrm{Zn^o}}$ stands for the diffusion coefficient of Zn°. Under this overestimating assumption, the charge would contain an extra term:

$$Q_{\mathrm{bound}} \approx \Delta t \left(\tfrac{3}{2} I_1 + \sum_{j=1}^{n_{\max}} I_j \right) \qquad (11)$$

Another voltammetric technique used here, the Linear Anodic Stripping Voltammetry (L-ASV) [13], consists in the application of a first deposition step at a constant potential followed by a linear scan of the potentials at a scan rate of 17 mV/s, moving from the deposition to the reoxidation potential.

4. Results and discussion

4.1 Observations

In order to proceed to a systematic discussion of the results, we summarize some regularities (despite increasing irreproducibility with higher concentrations) of a large number of experiments about the application of the simplest program of AGNES (see table 1) to concentrated solutions of Zn(II) in 7 observations:

- Observation 1: *For high concentrations, I is no longer proportional to* $[Zn^{2+}]$ *or* [Znº]. The calibrations of *I* vs $[Zn^0]$ (or $[Zn^{2+}]$) follow the linear behaviour expected and reported in previous works [2-4,6], but the linearity ceases at high concentrations. See, for instance, in Fig 1, how the calibration plot for the currents with $[KNO_3]$ =0.05 M (full triangle markers) bends at concentrations above $[Zn^0] \approx 4\times10^{-4}$ M (notice that [Znº] is a key parameter for the stripping stage). Given that the gain was 50, this corresponds to $[Zn^{2+}]\approx8\times10^{-6}$ M. The typical stripping current, predicted by the eqns. in appendix of ref. [1] and experimentally seen in previous AGNES literature, follows a fast decay, as the one shown by the reference line in the normalized currents plot (thick lines in Figs 2 and 3 or circle markers in Fig 4). In the anomalous stripping at high concentrations (see, for instance, Figs 2, 3, 4 and 5), there is a convex region of the stripping current (*I* vs t_2), which, for brevity we label here as "anomalous convex behaviour" (acb). Experiments with larger amounts of supporting electrolyte (e.g. 0.5

M) exhibit a less pronounced acb effect: see how in Fig 1, the linearity of the current -as commented above- is kept until $[Zn^0] \approx 4\times10^{-4}$ M for $[KNO_3]$ =0.05 M (full triangle markers), while for $[KNO_3]$ =0.5 M (full circle markers) the linearity is practically kept until $[Zn^0] \approx 0.05$ M (although for this [Zn°] the acb is observed, the current at t_2=200 ms approaches the expected value). The restoration of the standard stripping behaviour with higher ionic strength can also be seen in Fig 3.

• Observation 2: *Q is linear with* $[Zn^0]$ *for a much larger range than the intensity current measured at a given* t_2. The calibrations using charge (instead of the intensity current) as the response function of AGNES keep the linearity even at the concentrations for which *I*-plots bend (compare full and open markers in Fig 1). Linearity of the charge is not yet lost around $[Zn^0]\approx5\times10^{-3}$ M for $[KNO_3]$= 0.05M or at $[Zn^0]\approx0.2$ M for $[KNO_3]$= 0.5M. Obviously, the charge would no longer be useful when Zn° saturation is reached inside the drop. However, there is loss of linearity even before the computed saturation limit.

• Observation 3: *Sluggish stripping*. For huge concentrations, larger than those probed in Fig 1 (e.g. $[Zn^{2+}]$=0.016 M and *Y*=30 leading to [Zn°]= 0.48 M; see Fig 5), the initial recorded current is much less than expected (in Fig 4 see how the normalized currents denoted with diamond markers are below the reference curves depicted with circle markers). The current is initially almost "levelled-off" to a practically constant value for several seconds (see Fig 5) and, so, we call "sluggish stripping" to this acb variant or feature. This levelling-off effect appears (at high concentrations) when *Q* is still linear with $[Zn^0]$ and remains for larger concentrations. The levelling-off effect tends to decrease with increasing ionic strength.

• Observation 4: *Initial overcoming of the diffusion limited flux* (enhancement of the current or exaltation [22]). For intermediate-high concentrations , the anomalous stripping current is –at least at some points with short t_2- higher than the diffusion limited expected one (see upper curves in Figs 2, 3 and 4). Later in the stripping process (i.e. for longer t_2) the normalized representation (i.e. the experimental $\eta(t_2)$) becomes lower than the reference current (so that, from t_2=0 to t_2=50 s, the same charge is stripped off in all cases within the range where Q is linear with the concentration) as seen, for instance, in the diamond series in Fig 2 or 3. In order to experimentally confirm that the enhanced current of the first measured points is not the compensation of a very small initial current (at shorter stripping times than the first probed point), we have repeated some experiments with a shorter interval time (Δt=1 ms instead of the typical 50 ms value), and, we could see (Fig 4) that the enhanced currents are in operation from 1 ms onwards in this case. To confirm that the enhanced currents actually correspond to a stripping process faster (at some time of the stripping) than that of diffusion limited conditions, we have plotted in Fig 6 the normalized stripped charge $Q(t_2)/[Zn^0]= \eta_Q (t_2)$ in front of the stripping time: it is clearly seen that, say at t_2=0.5 s, the stripped charge of the series for Y=2 (square markers) even overcomes the upper bound computed with eqn. (11) (diamond markers).

The enhancement effect disappears for sufficiently high ionic strength and increases with a more positive stripping potential: see how in Fig 3 the exaltation is larger for $Y_2=10^{-12}$ than for $Y_2=10^{-8}$. For Cd, we have not found current enhancement with respect to diffusion limited conditions.

• Observation 5: *Longer deposition times can remediate the enhanced currents*. The anomalous convex behaviour with enhanced current, for intermediate-high concentrations of amalgamated metal, disappears at long deposition times t_1 as seen in Fig 2 (following the curves downwards, the deposition time increases and the currents eventually collapse with the thick reference line representing diffusion limited conditions).

• Observation 6*: Longer deposition times cannot remediate the sluggish stripping*. When dealing with huge [Zn⁰] (leading to observation 3), we have not found a trend of the recorded currents towards the reference curve when increasing the deposition time (see Fig 5).

• Observation 7: *Formation of powders and dendrites*. With the microscope, we have observed them around the surface of the mercury electrode using a deposition potential in the limit of diffusion all along the first stage of AGNES ($Y = 10^{10}$) leading to conditions close to saturation inside the amalgams. Calusaru and Kuta [23-25] have previously reported this kind of phenomenon for metals like Cu, Au and Cd in mercury. But, to our knowledge, such phenomenon has not yet been described for Zn. In general, we have observed that this phenomenon of deposition in a kind of external shell (or shield) is quite irreproducible, not only in the morphology of the dendrites, but also in the moment that it appears.

At ionic strength 0.05 M, the solid deposition can be detected visually at concentrations around $[Zn^{2+}] = 2\times10^{-2}$M . First, some bubbles appear, while at longer deposition times the formation of crystalline structures (dendrites) starts (see Fig 7). These dendrites

dissolve in the drop in some cases, while in other instances they grow becoming bigger and moving to the bottom of the drop, and leading occasionally to the falling of the drop. In the cases where we find solid deposition, the second stage shows the sluggish stripping phenomena.

In order to discard irreversibility of Zn as participant in the solid deposition on the Hg drops, we checked its appearance with Cd. We observed that the phenomenon of precipitation was more reproducible with Cd and that it happened at higher concentrations than for Zn, at $[Cd^{2+}]$=0.2 M. For Cd (data not shown), the process starts with the formation of a powder around the drop, followed by a movement which looks like a "boiling surface", where we can see the formation of some bubbles. At longer times a "shell" of dendrites is formed, with the ability to move around the drop. This can produce the loss of contact between the capillary and the drop.

4.2 Tentative interpretations

Shell formation of powders and dendrites (observation 7) was extensively explained in terms of a quantum effect of deposit without mechanical contact [23], but –as saturation is likely to be attained in our case- a simpler explanation is the solid deposit on precipitated Zn⁰ [24,25]. The 6 first observations of previous sub-section could arise from just one cause or from a combination of causes. We next discuss whether the 6 observations can be explained with just one cause, given that some observations are clearly connected (e.g. when acb appears due to either observation 3 or 4, there will be the loss of linearity described in observation 1) or some observations can be thought as variants of a general process (e.g. the enhanced stripping currents progressively tend – for higher Zn⁰ concentrations- towards the sluggish stripping behaviour, as seen in Fig

4, without a clear discontinuity in the morphology of the stripping curves). The list of considered hypothetical causes is:

i) Turbulence hypothesis. Convective flows in the amalgam can explain the intensity current exaltation.

ii) Electroneutrality limitation. The low ratio between the supporting electrolyte concentration and the active species concentration can result in a conductivity limitation.

iii) Irreversibility of Zn^0 reoxidation. This might explain the sluggish stripping.

iv) The "island" hypothesis. The formation of a biphasic amalgam (with crystals close to the surface) can produce exaltation or sluggish stripping.

v) The shell hypothesis. The formation of a shell around the drop can explain the sluggish stripping.

vi) Intermetallic formation. Impurities of Cu present in the mercury or in the solution could result in the formation of intermetallic compounds.

Given that hypotheses iii) to vi) are less plausible, they are discussed in the Appendix, while we focus here on the first two hypotheses.

i) The "turbulence" hypothesis [22,26-29]. Observation 4 requires some mechanism to produce currents larger than those yielded by diffusion limited conditions. Given that migration of Zn^0 has to be discarded because of its null charge, one should resort to convection. One might think, then, of a streaming flow inside the drop during the stripping stage. The driving force for this internal flow could be the dramatic change in density during the reoxidation of large concentrations of Zn^0 (perhaps interacting with the density gradient between the amalgams in the drop and in the capillary) or changes

in the surface tension. We could accept that under stagnant uniform conditions, the reoxidation might proceed without turbulence (despite the density gradient or other driving force), but any disturbance (let it be denoted with the generic name "seeds") might trigger the appearance of convective flows. These seeds could be remaining flows generated along the deposition step, remaining irregularities such as very small islands, patches of different surface tension, viscosity or potential or any other inhomogeneity. Once a small turbulence is initiated by a seed, it might suffer a kind of autocatalytic growth. Within this interpretative framework, if t_1 increases, the seeds disappear (more homogeneization) and the anomalous behaviour disappears (observation 5). Indeed, for larger deposition times, the streaming behaviour -in the stripping stage- would start later, due to the progressive extinction of seeds of streaming remaining from the deposition stage. The additional peak in Linear ASV experiments (see Fig 8 and the island hypothesis in the appendix for more details) could be due to such a convective transport.

Kolthoff and coworkers [22], reported that the streaming maxima tend to disappear at larger ionic strengths and interpreted this observation following von Stackelberg and Doppelfeld as the potential distribution being affected by the background electrolyte [27]. The screening effect of the capillary can result in an inhomogeneous electric field around the drop which would lead to the exaltation [30]. More recently, Islam *et al.* [26] reported visual confirmation of the streaming process in a HMDE. The lack of enhanced currents in Cd could be linked to the shorter distance between the stripping potential and the potential of zero charge [22,27] for Cd in comparison with Zn.

However, this hypothesis of internal turbulence cannot explain -without an additional phenomenon- observation 3 (levelling-off effect), because any amalgam turbulence always enhances the (initial) current.

ii) The electroneutrality limitation. When the potential is suddenly stepped from the deposition potential to the stripping potential, a huge amount of positively charged Zn^{2+} ions is delivered into the solution. One might think of a limitation in the supply of anions from the bulk of the solution to compensate for the released cations, thus producing an effective potential difference across the electrodic interfase which is quite different from the one applied, so that diffusion limited conditions inside the drop would not be achieved. This could explain the sluggish stripping seen at huge concentrations and its practical constancy during a relatively long period (observation 3). Further support comes from the observation that larger concentrations of supporting electrolyte favour (see Figs 1) the keeping of the linearity of the current, as commented above around observation 1 and the decreasing of the sluggish stripping (see Figs 3 and). The similarity of the sluggish stripping of Zn and Cd at comparable high concentrations also lends support to the origin of acb in electroneutrality. This explanation for the sluggish stripping (observation 3) matches theoretical and experimental results (on Tl) recently published [16,17] and could also imply that the potential relevant for the Nernstian equilibrium be different from the nominal applied potential. However, this mechanism of low medium conductivity cannot explain (at least straightforwardly) the current enhancement of observation 4 (for Zn) or why longer deposition times reduce them (observation 5) given that, for the stripping stage, we impose diffusion limited conditions inside the amalgam where migration cannot have any effect on Zn⁰ transport. In experiments with different stripping potentials, we

observed a larger current enhancement (with respect to the reference curve which corresponds to diffusion limited conditions inside the amalgam) for $Y_2=1\times10^{-12}$ than for $Y_2=1\times10^{-8}$ (see Fig 3). We speculate that with $Y_2=1\times10^{-12}$ a larger turbulence in the amalgam is produced, perhaps due to a migration turbulence in solution transmitted by mechanical contact to the amalgam, i.e. migration of Zn^{2+} away from the electrode would *induce* convection inside the amalgam, this also explaining why all acb effects disappear at sufficiently high ionic strength.

From the above discussion, it seems that a combination of causes is required to explain all the observations. A medium conductivity limitation (hypothesis ii) seems key, given the dramatic supression of the acb effect for sufficiently high ionic strength and a very reasonable explanation of observations 1 and 2. Moreover, the limitation of conductivity easily accounts for the sluggish stripping of observation 3 or levelling-off effect and observation 6. However, the currents higher than those of diffusion limited conditions in observation 4 require some enhancement mechanism, which is not inherent to an electroneutrality limitation. So, we could accept the turbulence hypothesis (i) as adequate and also likely to be involved in observation 5 as explained before: some homogeneization of the system with increasing deposition time might tend to desactivate the seeds of the turbulence (in the generic sense that includes potential or density inhomogeneities, islands, etc.). The lack of enhanced currents for sufficiently high ionic strength suggests the idea of the turbulences being induced (or maintained) by the migration of Zn^{2+} or by an inhomogeneous potential distribution.

Despite that the combination of the hypotheses of electroneutrality and (induced) turbulence can explain the observed observations, we stress the tentative character of all these speculations.

4.3 Practical strategies to overcome the anomalous convex behaviour

We aim now at providing an estimation of the conditions under which acb can be a problem for AGNES when the intensity current is taken as the response function. It is clear from what has been commented that the acb appears for high [Zn^{2+}] and low ionic strength. Indeed, we have seen how for ionic strength 0.05M, acb appears around [Zn^0]≈9×10^{-4} M, for a ionic strength 0.10M the acb started at [Zn^0]≈0.02 M and for a ionic strength 0.5M acb is seen at [Zn^0]≈0.05 M. However, for conditions before sluggish stripping, the acb can be remediated with longer t_1 (observation 5). As seen in Fig 2, for the same value of [Zn°]=Y[Zn^{2+}], we can have experiments with acb (such as the four upper curves) and experiments without acb (which act as reference, see thick line) just by changing the deposition time. Fig 10 classifies a large number of experiments (having reached the target condition of Nernstian equilibrium and absence of gradients by the end of the first stage) according to the observed acb through a visual inspection similar to that already described for Fig 2. Indeed, the procedure of plotting the normalised current (or $\eta(t_2)$) can serve as diagnosis of the acb. If acb is found, taking the faradaic current at a fixed t_2 as response function of AGNES is no longer valid.

Consistent with observations 1 and 5, we see in Fig 10 that acb predominates for higher [Zn°] and shorter times, while the standard behaviour for the stripping is seen for lower [Zn°] and longer deposition times. So, from a practical point of view, if a given

application of AGNES to a sample exhibits acb (diagnosed from the divergence of the sample measurement from the reference curve which can be obtained –for instance- in the calibration at not very high [Zn°]), one can choose to reduce Y, to increase t_1 or a combination of both.

Taking into account the results reported in this work, we detail below 4 strategies to apply AGNES in systems with a large Zn concentration and/or low ionic strength (i.e. when acb can appear or has been diagnosed):

a) Reduction of the prescribed preconcentration factor:

The reduction of Y is very easy to implement and very convenient, because the ensuing required deposition time (t_1) is proportionally reduced. Indeed, for gains below Y=5 and drop 1 in the HMDE, a deposition time of 50 s is more than sufficient –if other complications do not operate- to obtain the equilibrium goal. The only caution is that the response current has to be sufficiently higher than the blank to ensure a determination above the limit of quantification. We have previously reported the need of reducing the Y along metal titrations experiments of humic acid, when covering a wide range of metal concentration [8].

b) the use of the charge as response function:

Alternatively, in order to avoid acb, we can exploit observation 2. For those systems not exhibiting adsorption, the value of the stripped charge can be used as response function (instead of the faradaic current) as long as other phenomena of poor reproducibility do not appear. As seen in fig 11, Q is linear with the product of $[Zn^o]=Y\,[Zn^{2+}]$ for a range of experiments exhibiting or not acb (experiments from Fig 10) –being the slope, of

2.05×10^{-3} C M^{-1}, the value of the experimental η_Q. Thus, once more, we see that the charge can be useful even when the intensity current fails. This supports the practical possibility of using AGNES by taking Q as the response function: determining η_Q from calibration plots like Fig 11, measuring the charge in the sample and computing the free concentration with eqn (8). Shorter interval times (Δt) will lead to more accurate determinations of the charge.

c) the use of longer deposition times:

As commented above in subsection a), and in accordance with observation 5, there is a range of conditions (given by the analyte concentration, the desired gain and the ionic strength) where the increasing of the deposition time restores the linearity of the current response with Zn^{2+} concentration.

From diagram of Fig 10 we can formulate a rough rule of thumb, for ionic strength 0.05 M, of t_1 having to be

$$t_1 > 2\times10^5 \times Y \times \left[Zn^{2+} \right] \qquad (12)$$

in order to avoid acb. Of course, the application of this strategy is rather limited because the resulting "recommended" deposition time from the previous equation might be prohibitively long.

d) use higher ionic strength:

Increasing the ionic strength decreases the acb effect, thus enlarging the range of linearity for the current. So, when working with some synthetic solutions and large Zn concentrations, it might be easier to work with increased concentrations of background electrolyte. However, this strategy has also a limited use, given that for many samples,

the changing of the ionic strength can be critical (e.g. when measuring Zn in river water, the alteration of the ionic strength changes the speciation).

5. Conclusions

The standard application of AGNES to determine high Zn concentrations can be hindered by the anomalous convex behaviour (acb). This problem is more critical at lower ionic strengths, given that there is a trend towards the standard behaviour at sufficiently large concentrations of background electrolyte. The anomalous behaviour can be diagnosed by plotting the normalised current $\eta(t_2)$ along the stripping stage and comparison with a reference curve. We have described (section 4.1) a set of phenomena associated to this acb, such as the appearing of initial enhanced currents (with respect to the diffusion limited reference) or the sluggish stripping.

We speculate (see section 4.2) that the low conductivity in solution (which is also a levelling-off mechanism) and an induced turbulence can explain the previous observations regarding acb, but further work should elucidate this issue.

AGNES can be applied to determine high Zn concentrations, provided that care is taken to diagnose or circumvent the acb of the stripping currents. As strategies to avoid the loss of linearity in the current for high ratios of analyte concentration over background electrolyte concentration, we suggest (see section 4.3): a) the reduction of the applied gain; b) the use of the charge as response function (see also section 2); c) the use of longer deposition times (even if this is a limited measure) and d) use of higher ionic strength (also a limited measure).

Acknowledgments

Experimental help from Y. Diez is acknowledged. This work was financially supported by the Spanish Ministry of Education and Science (Projects CTQ2006-14385 and CTM2006-13583) and from the "Comissionat per a Universitats i Recerca del Departament d'Innovació, Universitats i Empresa de la Generalitat de Catalunya" and from the European Social Fund.

6. Appendix

We discuss here with more detail some of the hypotheses listed in section 4.2 which could participate in explaining the observations reported in section 4.1.

iii) The irreversibility hypothesis. There is a wealth of literature indicating that the system $Zn^o \rightarrow Zn(II)$ is irreversible. One objection to this being the cause of the observations 1 to 6 is that the applied reoxidation potential (E_2) is much more positive than E^o and irreversibility should decrease with the applied overpotential. Moreover, a very similar sluggish stripping has been observed for Cd (see Fig), which is an element considered to behave reversibly.

iv) The "island" hypothesis. Some authors [12,14] have considered the temporary formation of a "concentration inhomogeneity". One might think that -during the first moments of the deposition step- large amounts of Zn^o gather inside the amalgam close to the surface and form a kind of island in another phase or "association state". For instance, BenBassat et al. [13] interpreted the extra peaks in Linear Anodic Stripping Voltammetry (L-ASV) found with Cd as due to the reoxidation of such islands. We have repeated a similar experiment to that of BenBassat *et al*., with Cd and Zn and with

a deposition stage as that of AGNES (i.e. at a moderate *Y*). Our AGNES-like L-ASV voltammograms (Fig 8 and) for short deposition times exhibit what could be called an extra peak. Thus, our results in these figures could be consistent with this hypothesis by explaining that when t_1 is very long, the island -which is metastable- disappears[15]. In this way, we could understand observation 3 (sluggish stripping) as a kind of kinetic limitation of the re-dissolution of the island (analogous to that seen in fig. 8 of ref. [31]), and we could explain observation 4 (enhanced currents) as part of the deposited Zn⁰ being closer to the surface, but some other phenomenon must be involved, given that the existence of the islands can be invoked both to explain the slowing down and the speeding up of the standard stripping. Be as it may, observation 2 (*Q* being correct for concentrations when the enhanced currents occur) indicates that AGNES conditions have been attained, so we need to accept that the desired Zn⁰ concentration has been attained uniformly inside the drop at the fixed value $Y[Zn^{2+}]$. If there were other phases or compounds, we would record larger charges for longer t_1 (and we have seen this is NOT the case in many experiments; e.g. in 2 or 5). To render the island hypothesis compatible with the experimentally found charge corresponding to AGNES requirements, we would need to accept that some Zn⁰ is converted into a form which counts for the total activity inside the drop, but with very different availability for different experiments.

v) The shell hypothesis. The optical observation of a shell around the mercury drop, described in observation 7, suggests the possibility of existence of similar shells for lower concentrations (despite we have not been able to see them with our microscope). The sluggish stripping, observation 3, could be explained by assuming that a shell of Zn⁰ and/or other materials gathers -without mechanical contact with Hg, so that

observation 2 holds- around the drop hindering the stripping. First objection: why does this hypothetical shell not hinder the deposition stage?. Another objection: the enhancement seen in observation 4 cannot be explained by this hypothesis. A third objection to this hypothesis is that this shell effect should imply the usually large initial reoxidation current (collapsing with the reference curve) at very short stripping times (because diffusion in the thin solution layer in between the drop and the shell would not be initially hindered) which has not been observed .

vi) Intermetallic formation. The formation of intermetallic compounds of Zn and Cu could produce a decreased AGNES intensity current (sluggish stripping), given that it is well known that more positive potentials than those actually applied (close to that of Cu°) are required for their reoxidation [32]. From the maximum declared content of Cu° in the used polarographic mercury (5×10^{-6}%), one estimates $[Cu^0]_{\text{from amalgam}} = 1\times10^{-5}$ M. To this amount one should add the Cu° deposited from the solution which will depend on the used [KNO_3] and deposition time the KNO_3. From the maximum content of Cu in KNO_3 declared by the supplier (5×10^{-7}%), we compute a typical $[Cu^{2+}]\approx10^{-9}$ M, from which the deposited concentration can be estimated as

$$[Cu^0]_{\text{from solution}} = \frac{D_{Cu^{2+}}\left[Cu^{2+}\right]4\pi r_0^2}{\delta \,{}^4\!/_3\, \pi r_0^3} t_1 \approx 5\times10^{-10}\ \text{M} \qquad (13)$$

where δ is the diffusion layer thickness (around 2×10^{-5} m) and t_1 is taken around 1000 s. We conclude that the amount of Cu° coming from the solution is negligible in front of the one in the amalgam, but, in turn, $[Cu^0]_{\text{from amalgam}}$ is negligible in front of the [Zn°] concentrations used when the linearity of AGNES response is lost. Given that in our experiments $[Zn^0] >> [Cu^0]_{\text{from amalgam}}$, the most likely intermetallic compounds to interfere in AGNES measurements are CuZn or $CuZn_3$ (the most unfavourable case)[33]. As AGNES intensity current (or charge) depends on [Zn°] and its variation,

due to the possible formation of intermetallic compounds, is negligible ($3\times[Cu^0]<<[Zn^0]$), we conclude that –for these cases- their formation cannot explain the sluggish stripping. We can even argue more directly noting that –if Cu^0 coming from solution is negligible-, once all Cu^0 (from amalgam contamination) becomes the intermetallic $CuZn_3$, the accumulation of Zn^0 will proceed along the first stage of AGNES until $[Zn^0]$ will reach the desired $Y[Zn^{2+}]$ and –given that $CuZn_3$ is not reoxidized at the used stripping potentials for Zn^0- the response function will be the same as if Cu was not present. Work is in progress in our laboratory to study the impact of intermetallic compounds on AGNES.

Table

Table 1: Simplest potential program of AGNES.

potential	deposition at E_1 for prescribed gain (Y)	deposition at E_1 (rest period)	E_2 in stripping or second stage (gain Y_2)
time	t_1-t_w	t_w	t_2
stirring	on	off	off

608

609 ## Figures

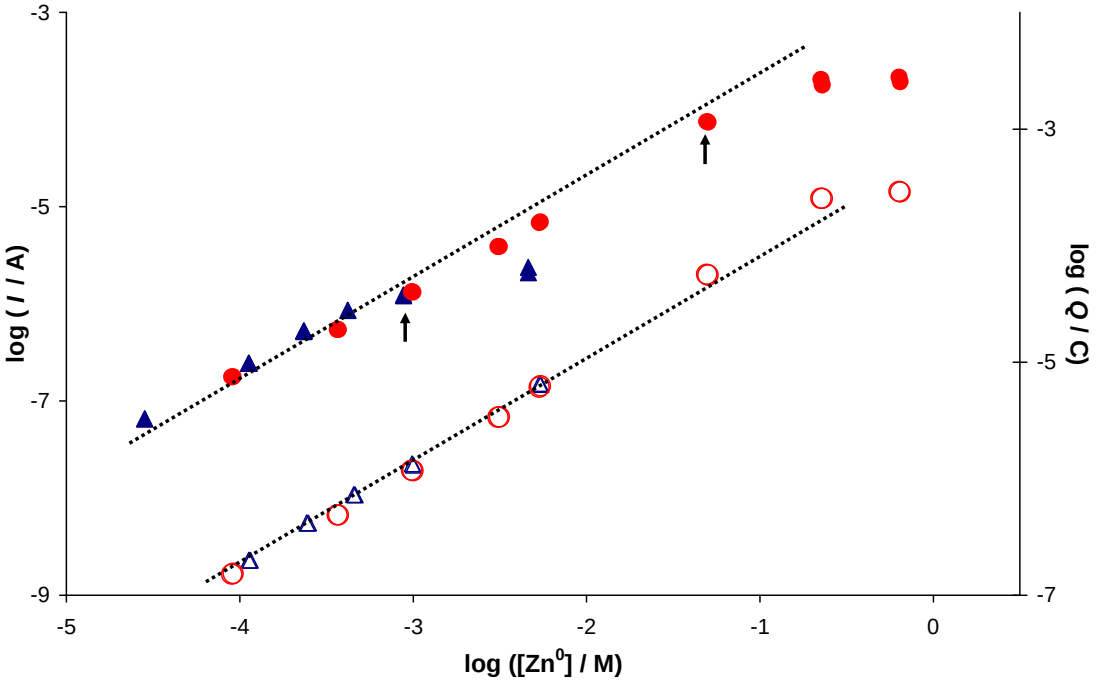

610

611

612 Fig 1: Calibration plot of the logarithm of the faradaic current (full markers referred to
613 the left axis) and of the logarithm of the charge (open markers referred to the right axis)
614 vs. Zn concentration inside the amalgam. I is measured at t_2=200 ms, while Q is
615 computed with Δt= 50 ms in eqn. (9). Makers: triangle for [KNO_3]=0.05 M and circle
616 for [KNO_3]=0.5 M. Settings: Y= 50; t_1= 400 s ; t_w=50 s. The arrows indicate the first
617 concentration of each [KNO_3] which clearly exhibits acb (via an analysis as that
618 performed in Fig 2) and also corresponds to the loss of linearity of current in this
619 calibration plots. The dotted straight lines are lines of slope 1 as expected from eqn. (4).

620

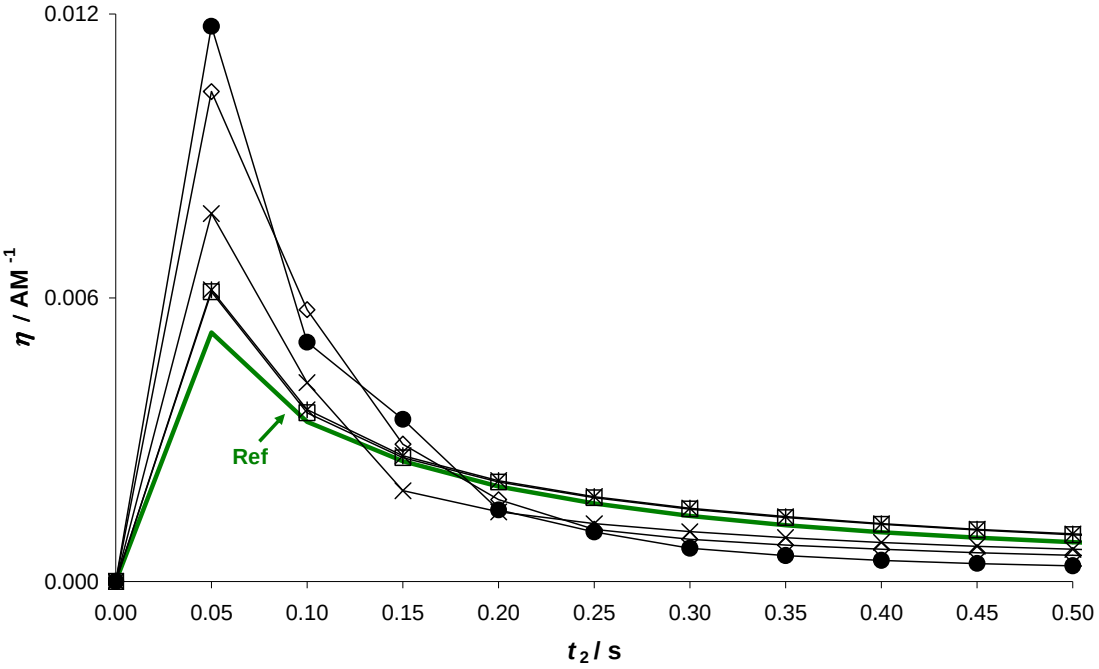

621

622 Fig 2: Plot of the normalised current $\eta(t_2) = \frac{I(t_2)}{Y\left[\mathrm{Zn}^{2+}\right]}$ -see eqn. (3)- showing how the

623 anomalous convex behaviour in the stripping current decreases with increasing

624 deposition time. Markers for experimental data: (•) t_1=400s, (◊) t_1=800s, (×) t_1=1200s,

625 (□) t_1=2000s and (∗) t_1=2200s. Other conditions: $[Zn^{2+}]=1.3\times10^{-5}$ M; Y=50; [Zn°]=

626 6.5×10^{-4} M, $[KNO_3]$=0.1M. The thick line indicates the "reference" (or typical)

627 stripping decay, which has been achieved with $[Zn^{2+}] = 3.0\times10^{-6}$ M, Y=50.

628

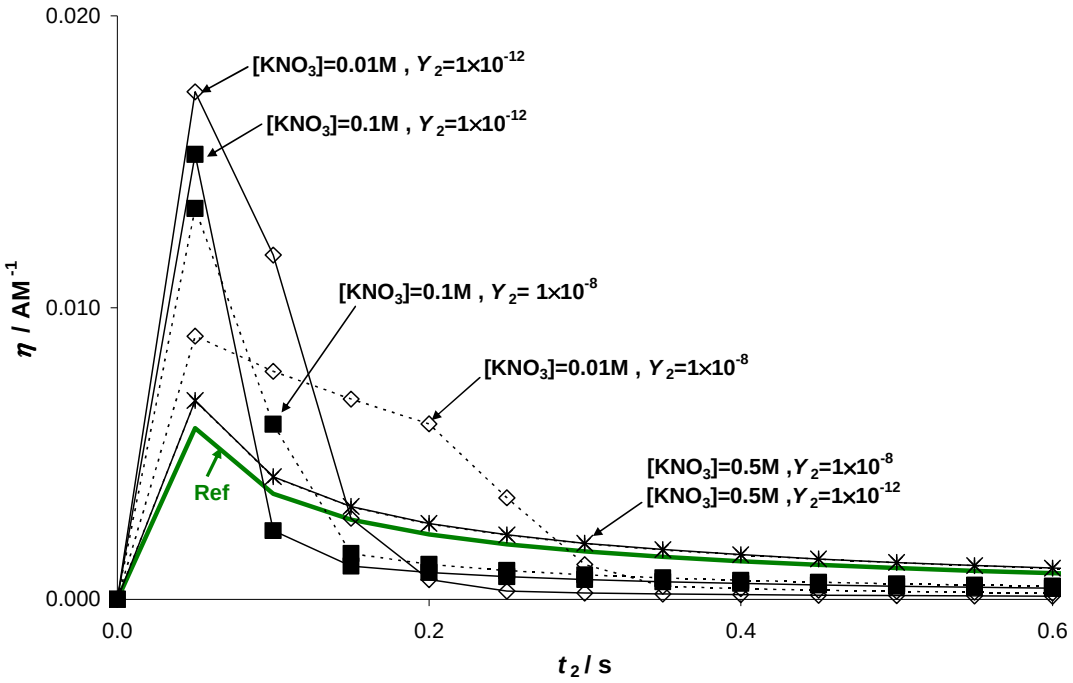

Fig 3: Plot of the normalised currents vs. t_2 for $[Zn^{2+}]= 5.8\times10^{-5}$M, different stripping potentials E_2 and $[KNO_3]$. Markers for experimental data: (—) E_2=-0.5956V, -0.6025V and -0.6102V for $[KNO_3]$=0.01M, 0.1M and 0.5M respectively, corresponding to $Y_2=1\times10^{-12}$; (---)E_2=-0.7139V, -0.7208V, -0.7285V for $[KNO_3]$=0.01M, 0.1M and 0.5M respectively, corresponding to $Y_2= 1\times10^{-8}$; (◊) $[KNO_3]$= 0.01M; (■) $[KNO_3]$= 0.1M; (∗) $[KNO_3]$= 0.5M. Settings: t_1=400s, t_w=50s, Y=50, [Zn°]= 2.9×10^{-3}M. The thick line indicates the reference stripping decay obtained with Y=1.

638

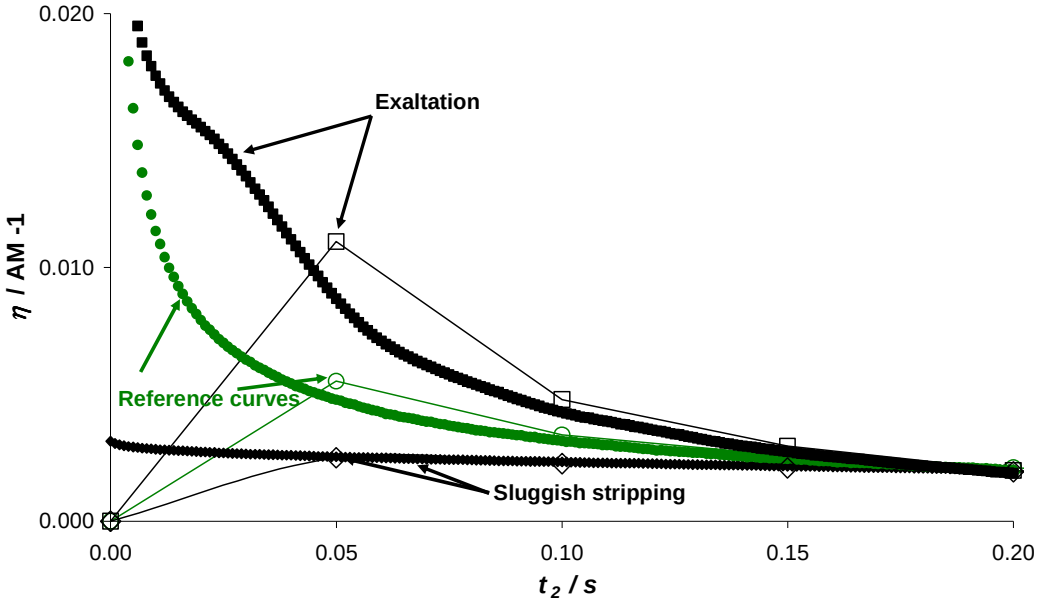

639

640 Fig 4: Plot of the normalized current η vs. t_2 showing the two types of acb: exaltation
641 (square marker) and sluggish stripping (diamond marker) compared with a reference
642 curve (circle marker). Open markers indicate sample time Δt= 50 ms and full markers
643 indicate Δt=1 ms. Parameters: (o)Y=1, t_1= 50 s, Δt= 50 ms; (•) Y=1, t_1= 50s, Δt=1 ms;
644 (□) Y=2, t_1= 50s, Δt= 50 ms; (■)Y=2, t_1= 50s, Δt=1 ms; (◊) Y=50, t_1= 400s, Δt= 50 ms;
645 (♦)Y=50, t_1= 400s, Δt=1 ms. Settings: $[Zn^{2+}] = 1.90\times10^{-4}$M, $[KNO_3]$=0.01M, t_w=50s.

646

647

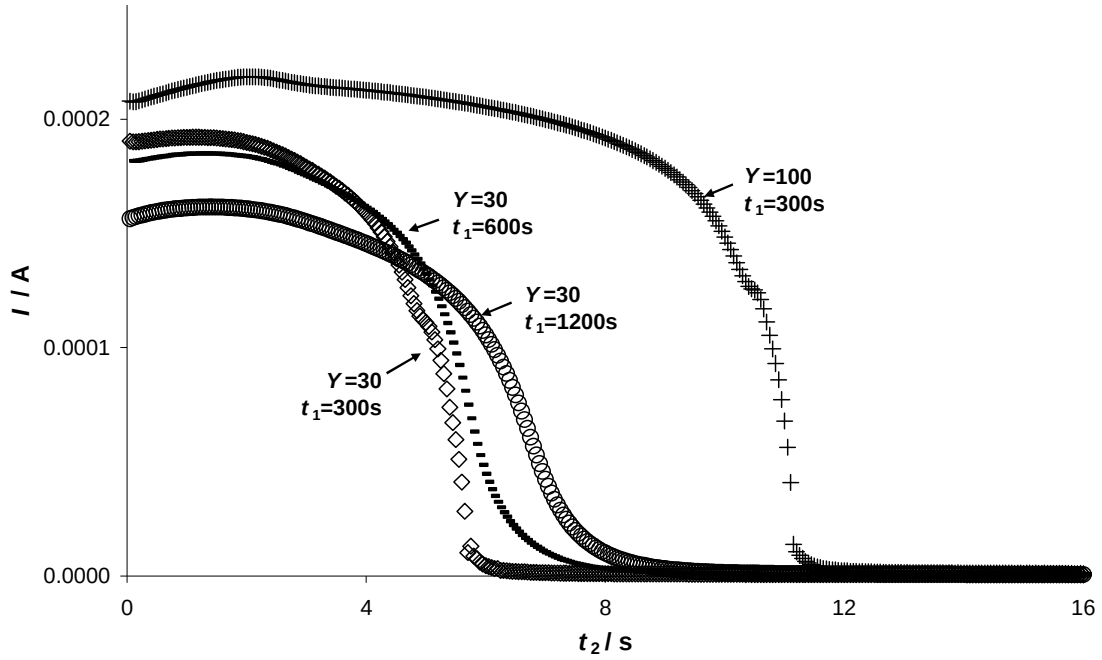

Fig 5: Plot showing the sluggish stripping currents for huge concentrations. Y=30 (several deposition times: (◊), t_1=300s,(–) t_1= 600s (o) and t_1=1200s) and Y=100 ((+) t_1=300 s). Settings: $[Zn^{2+}]=1.36\times10^{-2}$ M; $[KNO_3]$=0.05M.

653

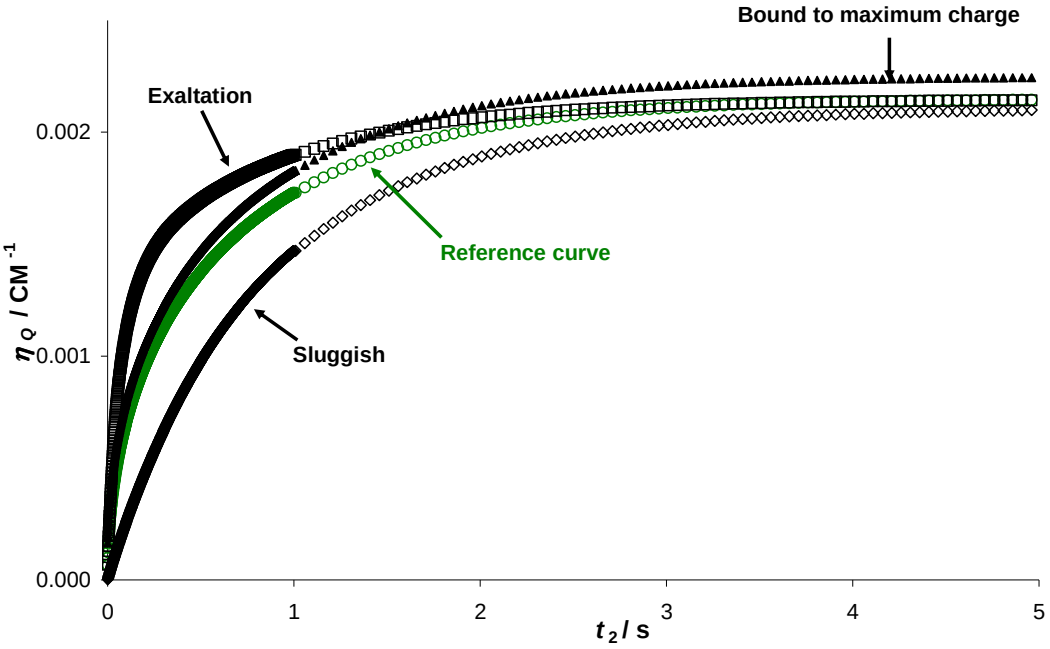

654

655 Fig 6: Plot of the normalized charge η_Q (see eqn. (7)) vs. t_2 for the data of Fig 4 (same
656 markers) with Δt=1 ms for the first second of the stripping. The curve that is always
657 below the reference curve is classified as sluggish stripping while the curve that –at
658 some point- overcomes the reference one is classified as corresponding to enhanced
659 currents. The exaltation even overcomes the solid triangle series that stands for the
660 maximum expected charge (under diffusion limited conditions) computed applying eqn.
661 (11) to the data of the reference experiment.

662

663

664 a) b)

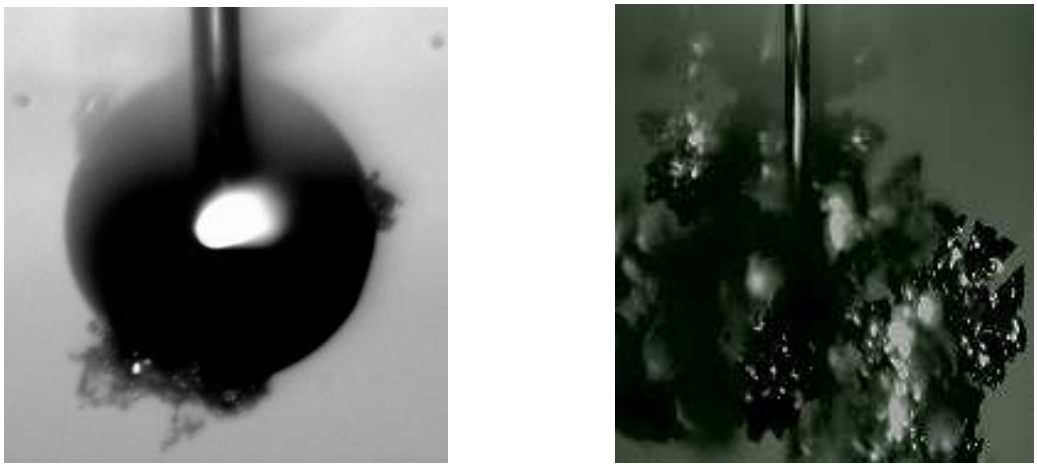

665

666

667 Fig 7: Photographs of the mercury drop electrode obtained in an AGNES experiments
668 with diffusion limited deposition potential ($Y = 10^{10}$) at [KNO_3] = 0.05 M. a) [Zn^{2+}] =
669 3.76×10^{-2}M and t_1 = 400s. b) [Zn^{2+}] = 2×10^{-2}M and t_1 = 1800s

670

671

672

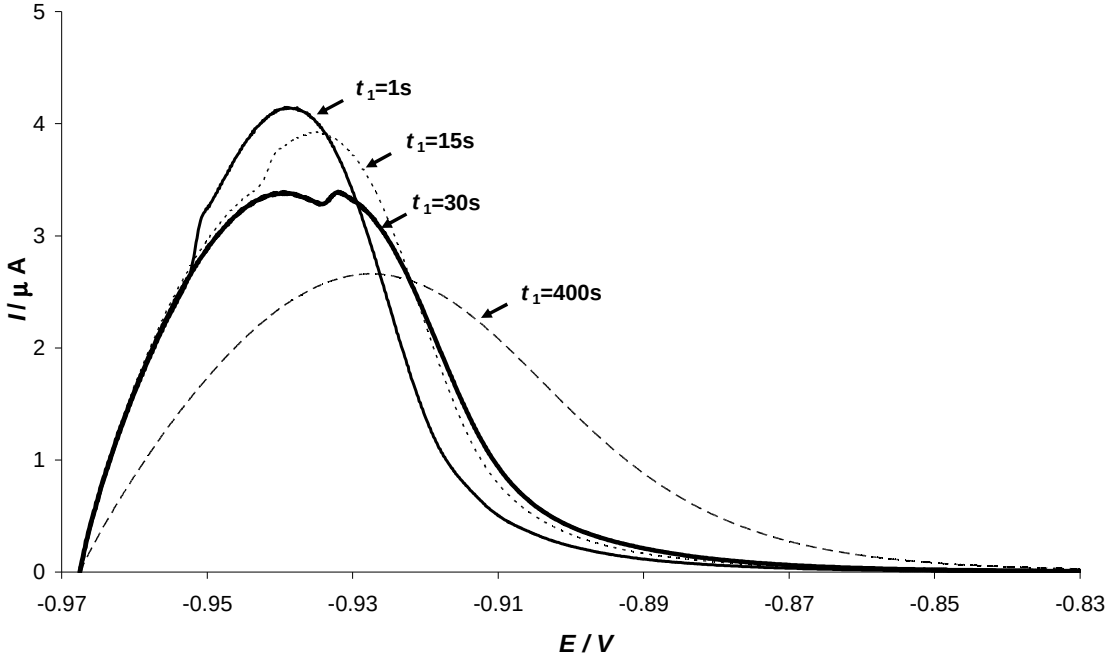

673

674 Fig 8: Linear Anodic Stripping Voltammogram (L-ASV) of a solution with
675 $[Zn^{2+}]=4.81\times10^{-3}$M and several deposition times. Thin continuous line t_1= 1s, thin
676 dotted line t_1= 15s, thick continuous line t_1= 30s, dashed line t_1= 400s. Deposition stage
677 with Y=1. Linear stripping with scan rate: 17 mV/s and ΔE= 0.15 mV, [KNO_3]= 0.05M.

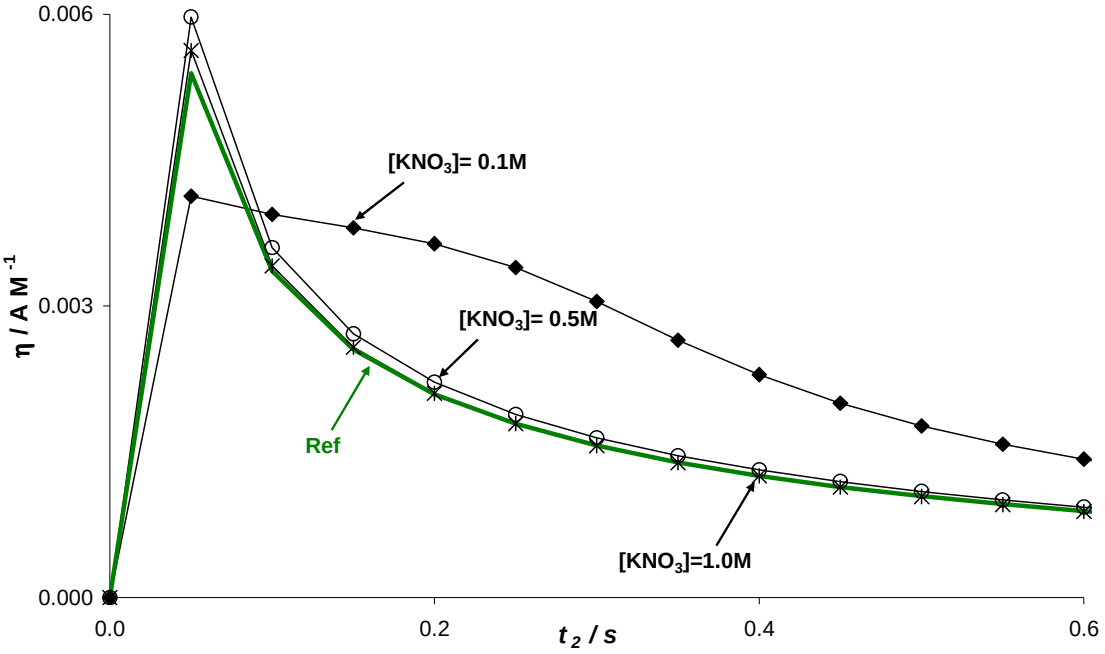

678

679 Fig 9: Plot of η vs. t_2 for Cadmium with different ionic strengths . Parameters: $[Cd^{2+}]=$

680 3.2×10^{-3}M, Y=12, (♦) $[KNO_3]$=0.1M and t_1= 400s; (o) $[KNO_3]$=0.5M and t_1=1200s; (∗)

681 $[KNO_3]$= 1.0M and t_1= 400s. Reference curve: $[Cd^{2+}]= 3.2\times10^{-3}$M , Y=8, t_1= 400s.

682

683

684

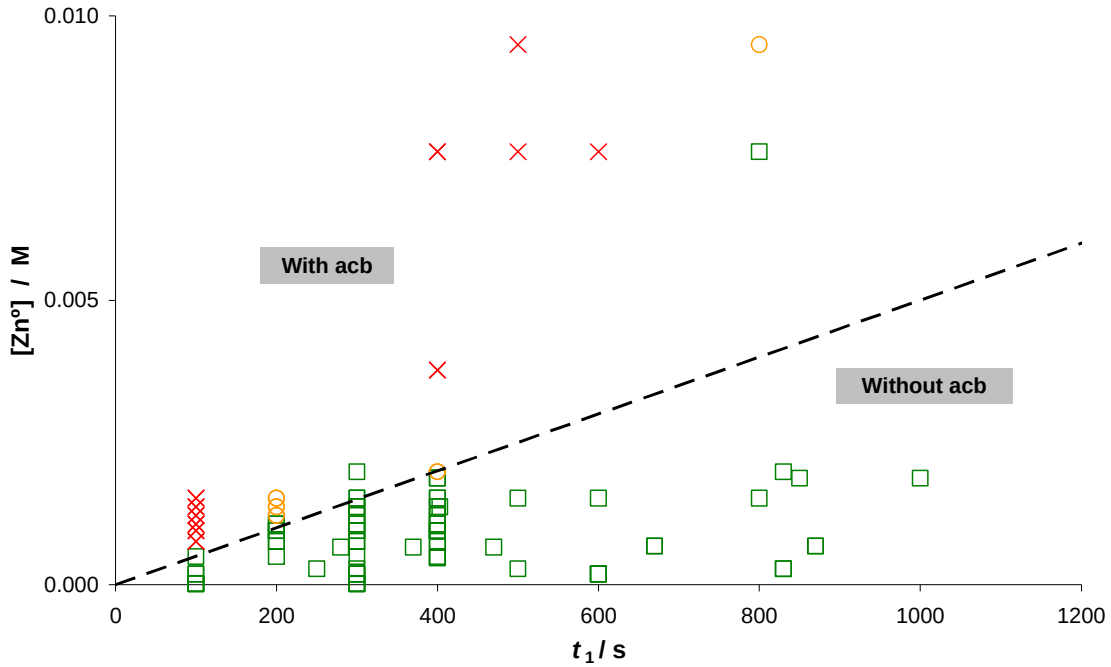

685

686 Fig 10: Nomograph indicating the appearance of the acb in the stripping stage for
687 different combinations of the product Y [Zn^{2+}] (i.e. aimed [Zn°]) and deposition times
688 (t_1) in the simplest potential program of AGNES for more than 50 experiments with
689 various Zn^{2+} concentrations, [KNO_3]= 0.05M. Markers: (□) curve indicates experiments
690 where acb effect was not detected; (×) indicates experiments where acb could be clearly
691 identified; (o) indicate experiments where the acb effect (if existent) was very mild.

692

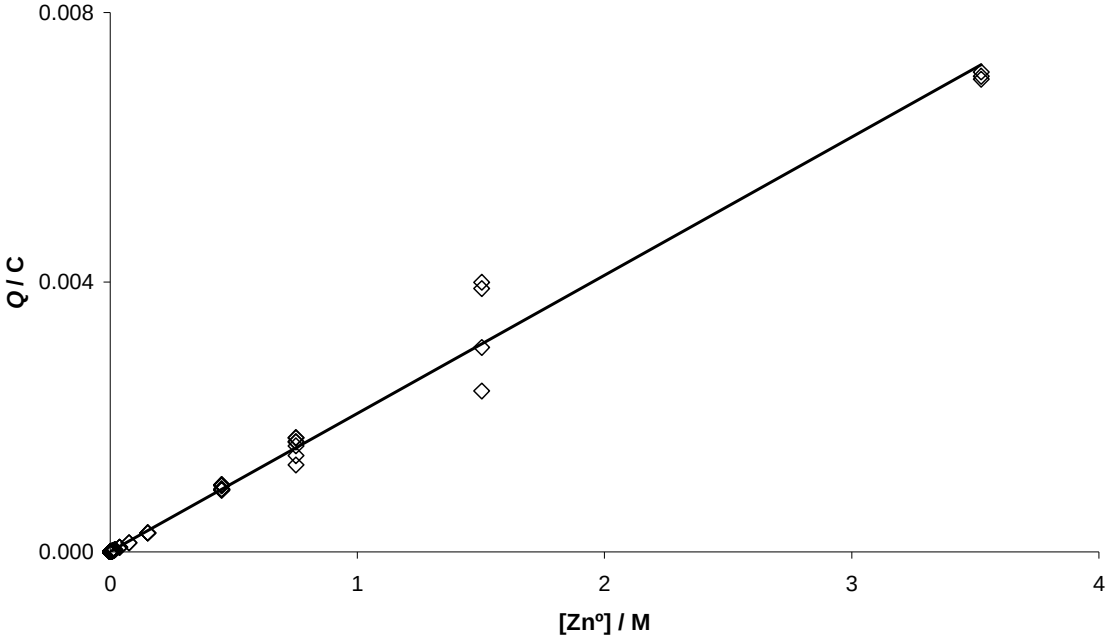

693

694 Fig 11: Plot of the total stripped charge (Δt= 50 ms in eqn. (9)) vs. [Zn°]=Y[Zn^{2+}] for the
695 same experiments analyzed in fig 10 and a few more at higher concentrations. The slope
696 of the line (2.05×10^{-3} C/M) is the factor η_Q which can be used together with the
697 measured charge when the acb affects the faradaic current.

698

699

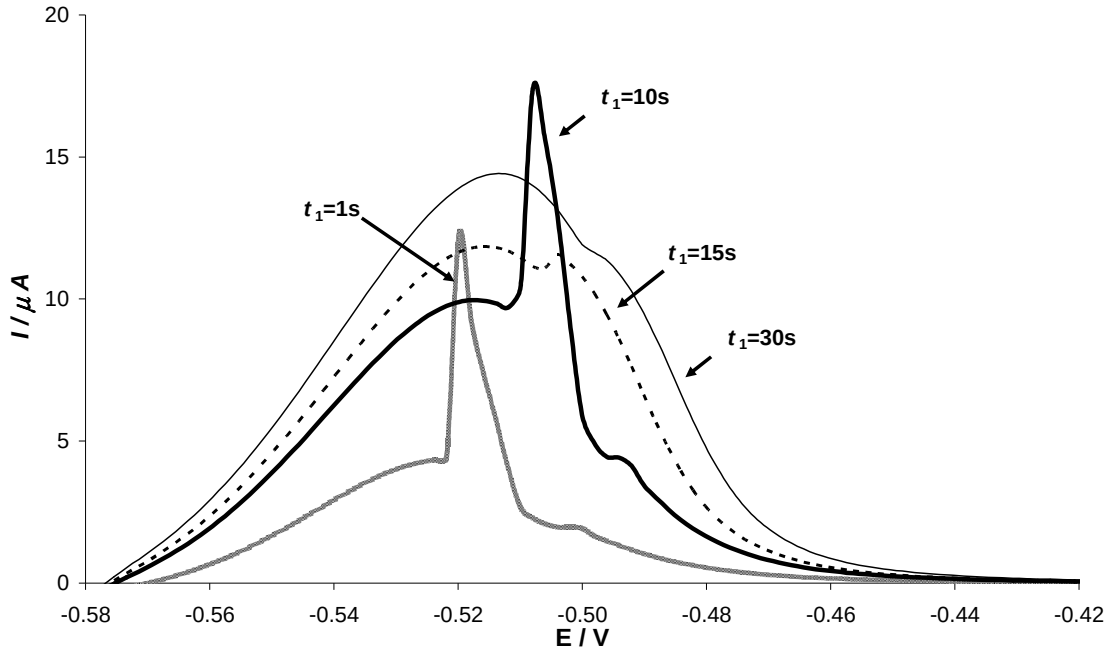

700

701 Fig 12: Linear Anodic Stripping Voltammogram (L-ASV) of a solution with $[Cd^{2+}]$=
702 1.34×10^{-3}M. Deposition potential corresponding to Y=20. Deposition times: (---) t_1=
703 1s; (**━**) t_1= 10s: (**━ ━**) t_1= 15s; (–) t_1= 30s. Linear stripping with scan rate: 0.017V/s and
704 ΔE= 0.00015V. $[KNO_3]$= 0.05M.

705

706 ## References

707

708

709 [1] J.Galceran, E.Companys, J.Puy, J.Cecília, J.L.Garcés, J. Electroanal. Chem. 566
710 (2004) 95.

711 [2] E.Companys, J.Cecília, G.Codina, J.Puy, J.Galceran, J. Electroanal. Chem. 576
712 (2005) 21.

713 [3] E.Companys, J.Puy, J.Galceran, Environ. Chem. 4 (2007) 347.

714 [4] E.Companys, M.Naval-Sanchez, N.Martinez-Micaelo, J.Puy, J.Galceran, J. Agric.
715 Food Chem. 56 (2008) 8296.

716 [5] Domingos R.F., C.Huidobro, E.Companys, J.Galceran, J.Puy, J.P.Pinheiro, J.
717 Electroanal. Chem. 617 (2008) 141.

718 [6] J.Galceran, C.Huidobro, E.Companys, G.Alberti, Talanta 71 (2007) 1795.

[7] C.Huidobro, E.Companys, J.Puy, J.Galceran, J.P.Pinheiro, J. Electroanal. Chem. 606 (2007) 134.

[8] J.Puy, J.Galceran, C.Huidobro, E.Companys, N.Samper, J.L.Garcés, F.Mas, Environ. Sci. Technol. 42 (2008) 9289.

[9] L.S.Rocha, E.Companys, J.Galceran, H.M.Carapuca, J.P.Pinheiro. Evaluation of thin mercury film rotating disc electrode to perform Absence of Gradients and Nernstian Equilibrium Stripping (AGNES) measurements. Submitted to Talanta, 2009;

[10] L.A.Zabdyr, C.Guminski, J. Phase Equilib. 16 (1995) 353.

[11] A.Arevalo, J.Acosta, Anales De Quimica 70 (1974) 478.

[12] J.Buffle, Arch. Sci. (Genève) 22 (1969) 393.

[13] A.H.I.Benbassat, A.Azrad, Electrochim. Acta. 23 (1978) 63.

[14] Z.Galus, L.Meites, Crit. Rev. Anal. Chem. 4 (1975) 359.

[15] J.P.Dumas, L.Bougarfa, J.Bensaid, J. Physique 45 (1984) 1543.

[16] I.Streeter, R.G.Compton, J. Phys. Chem. C 112 (2008) 13716.

[17] J.G.Limon-Petersen, I.Streeter, N.V.Rees, R.G.Compton, J. Phys. Chem. C 112 (2008) 17175.

[18] A.I.Vogel, Textbook of Quantitative Chemical Analysis, 6th ed., Pearson Education, Harlow, 2000.

[19] M.P.Bradshaw, P.D.Prenzler, G.R.Scollary, Electroanal. 14 (2002) 546.

[20] M.T.Vasconcelos, M.Azenha, V.de Freitas, Analyst. 125 (2000) 743.

[21] M.L.Tercier, C.Bernard, F.Bujard, S.Rodak, J.Buffle, Electroanal. 2 (1990) 89.

[22] Y.Okinaka, I.M.Kolthoff, T.Murayama, J. Amer. Chem. Soc. 87 (1965) 423.

[23] A.Calusaru, J.Kuta, Nature 211 (1966) 1080.

[24] A.Calusaru, Electrochim. Acta. 12 (1967) 1507.

[25] A.Calusaru, J.Kuta, J. Electroanal. Chem. 20 (1969) 383.

[26] M.M.Islam, T.Okajima, T.Ohsaka, Electrochem. Commun. 6 (2004) 556.

[27] H.H.Bauer, Electroanal. Chem. 8 (1975) 169.

[28] M.Noufi, C.Yarnitzky, M.Ariel, Electroanal. 8 (1996) 836.

[29] M.S.Saha, T.Okajima, T.Ohsaka, J. Phys. Chem. B 106 (2002) 4457.

749 [30] J.Heyrovský, J.Kuta, Principles of Polarography, Academic Press, New York,
750 1966.

751 [31] S.Belcadi, J.Bensaid, L.Bougarfa, J.P.Dumas, A.Jouanneau, J. Physique 43
752 (1982) 945.

753 [32] T.R.Copeland, R.A.Osteryoung, R.K.Skogerboe, Anal. Chem. 46 (1974) 2093.

754 [33] C.Guminski, Z.Galus, Intermetallic compounds in mercury, Pergamon Press,
755 Oxford (UK), 1992.
756
757